The Journal of Antibiotics (2017) 70, 871–877

www.nature.com/ja

ORIGINAL ARTICLE

Verification of oligomycin A structure: synthesis and biological evaluation of 33-dehydrooligomycin A

Lyudmila N Lysenkova[1], Oleg Y Saveljev[2], Natalya E Grammatikova[1], Vladimir B Tsvetkov[3,4,5], Olga B Bekker[6], Valery N Danilenko[6], Lyubov G Dezhenkova[1], Eugene E Bykov[1], Olga A Omelchuk[1], Alexander M Korolev[1] and Andrey E Shchekotikhin[1,7]

Although, the structure of oligomycin A (1) was confirmed by spectroscopic and chemical evaluations, some crystallographic data cast doubt on the originally adopted structure of the side 2-hydroxypropyl moiety of this antibiotic. It was suggested that the side chain of the oligomycin is enol-related (2-hydroxy-1-propenyl). To clarify this matter we synthesized and evaluated 33-dehydrooligomycin A (2) prepared by the Kornblum oxidation of 33-*O*-mesyloligomycin A (3) by dimethyl sulfoxide. NMR data for 33-dehydrooligomycin (2) and results of quantum chemical calculations have shown that this derivative exists in the keto rather than in the enol tautomer 2a. The *in vitro* antimicrobial activity of 2 was approximately two times weaker in comparison with oligomycin A against *Streptomyces fradiae* ATCC-19609 and reference *Candida* spp. strains and similar activity against certain filamentous fungi. The docking binding estimate of 2 with F_OF_1ATP synthase showed a slight decrease in binding affinity for 2 when compared with oligomycin A; that correlated with its activity against *S. fradiae* ATCC 19609 that is supersensitive to oligomycin A. The *in vitro* antiproliferative activities of 2 are also discussed.
The Journal of Antibiotics (2017) **70,** 871–877; doi:10.1038/ja.2017.48; published online 19 April 2017

INTRODUCTION

The macrolide antibiotic oligomycin A was discovered in 1954.[1] It is a well-known inhibitor of the F_O part of H^+-ATP synthase and widely used for investigation of the mitochondrial F_1F_O-ATPase. Notable results have been published by Symersky *et al.*,[2] in which detailed research of the high-resolution (1.9 Å) crystal structure of oligomycin A bound to the subunit c_{10} ring of the yeast mitochondrial ATP synthase was used. They highlighted a mechanism of inhibition of ATP synthase by oligomycin A, indicating that the binding of the macrocyclic antibiotic with the c-ring of the ATPase positioned at the proton channel led to inhibition of proton translocation as a result of blocking the access of protons to the carboxyl group of Glu59.[2]

The structure of the oligomycin A (**1**) (Figure 1) has been evaluated by the NMR–electrospray ionization (ESI) mass spectrometry and by investigation and comparison of its chemical degradation products with those derived from oligomycin B.[3–5] Similarly, the total asymmetric syntheses of related antibiotics of this family—rutamycin B and oligomycin C—were carried out.[6] According to earlier researches, nearly all the antibiotics of oligomycin–rutamycin group have 2-hydroxy-propanol side chain in the spiroketal part of the molecule (Supplementary Figure S1).

Recently, however, crystallographic studies of oligomycins performed by Palmer *et al.* cast doubt on the originally adopted structure of oligomycin A (**1**) with the 2-propanol side chain (R). In 2008 and 2013, Palmer *et al.* presented X-ray data for two crystal forms of oligomycin A (isolated from *Streptomyces diastatochromogenes*[1] and *S. diastaticus*[7])[8–10], that indicated that the side chain of oligomycin A was as enol-related group, 2-hydroxy-1-propenyl (**2a**) (Figure 1).

Although our studies were directed at the development of methods of transformations of oligomycin A (isolated from *Streptomyces avermitilis*), they clearly confirmed its structure with the 2-propanol side chain (**1**).[11–14] Palmer's surprising data prompted us to initiate additional chemical verification of the structures of the oligomycin A side chain. Interestingly, in the Handbook of Berdy *et al.*,[15] the oligomycin A was originally described with a propanone side chain as structure (**2**) (Figure 1), but we did not find any other original studies concerning the structure assignments or biological characterizations of oligomycins with ketone (**2**) or enol (**2a**) groups in the side chain. Thereby, we have for the first time described the synthesis, structural studies and biological evaluation of an oligomycin A analog with propanone side chain—33-dehydrooligomycin A (**2**).

RESULTS

Synthesis

We have started these studies with the development of a way to transform oligomycin A (**1**) into 33-dehydrooligomycin A (**2**). All

[1]G. F. Gause Institute of New Antibiotics, Moscow, Russian Federation; [2]M. V. Lomonosov Moscow State University, Moscow, Russian Federation; [3]A. V. Topchiev Institute of Petrochemical Synthesis, Russian Academy of Sciences, Moscow, Russian Federation; [4]Institute for Physical-Chemical Medicine, Moscow, Russian Federation; [5]Research Institute of Influenza, St-Petersburg, Russian Federation; [6]N. I. Vavilov Institute of General Genetics, Russian Academy of Sciences, Moscow, Russian Federation and [7]D. I. Mendeleev University of Chemical Technology of Russia, Moscow, Russian Federation
Correspondence: Dr LN Lysenkova, G. F. Gause Institute of New Antibiotics, B. Pirogovskaya 11, Moscow 119021, Russian Federation.
E-mail: lyudmil-lys@yandex.ru
Received 24 November 2016; revised 27 January 2017; accepted 23 February 2017; published online 19 April 2017

attempts to find the direct method of oxidation of 2-propanol side chain of **1** were unsuccessful. We were unable to perform the transformation of **1** into **2** by CrO_3, TAPI, Swern oxidation or any other method, probably because of low selectivity of this oxidizer or high reactivity of dienic system of the macrocycle. Previously, a selective method of activation of 33-hydroxyl group in the side chains of oligomycin A (**1**) by transformation into 33-*O*-mesyloligomycin A (**3**) had been discovered.[12] We did check an opportunity for the conversion of 33-*O*-mesylate **3** into **2** by the Kornblum oxidation reaction.[16] The mechanism of the conventional Kornblum oxidation involves oxysulfonium ion formation that undergoes elimination in the presence of bases into the carbonyl compound.[17] We have found that triethylamine can be efficient as a base for this reaction despite the instability of the oligomycin macrocycle in the presence of the base.[18] Treatment of **3** with triethylamine in dimethyl sulfoxide (DMSO) at 105 °C for 3–4 h led to 33-dehydrooligomycin A (**2**) (Scheme 1). The raw product was purified by column chromatography and then crystallized from the mixture of hexane–dichloromethane (10:1) that gave 33-dehydrooligomycin A (**2**) in 50% yield with 96.1% purity (Supplementary Figure S2). HPLC analysis has shown that **2** is totally different from oligomycin A by its retention time in HPLC analysis. The Rt (retention time) for oligomycin A was 15.13 min, whereas that for 33-dehydrooligomycin (**2**) was 16.58 min (Supplementary Figure S3).

Structure confirmation

The structural elucidation of **2** was developed by HRMS ESI, 1D and 2D NMR experiments, IR and UV spectroscopy (Supplementary Table S1 and Supplementary Figures S2 and S4–S10). No significant changes were noticed in the IR spectrum (Supplementary Figure S4). The pseudo-molecular ions $[M+Na]^+$ were recorded as *m/z* 811.4988 corresponding to a formula of $C_{45}H_{72}O_{11}Na$ and $[M+K]^+$ as *m/z* 827.4763 corresponding to a formula of $C_{45}H_{72}O_{11}K$ (Supplementary Figure S5). The total quantity of carbon atoms detected by ^{13}C NMR spectrum corresponded for the molecular formula of 33-dehydrooligomycin (**2**) to be $C_{45}H_{72}O_{11}$. The structure of **2** was established by analyzing its NMR data in comparison with starting oligomycin A (**1**) and 33-*O*-mesyloligomycin A (**3**).

In the NMR spectra of oligomycin A (**1**) and its mesylate **3** signals of the 33-CH group, δC 64.6 p.p.m. (δH 4.00 p.p.m.) and δC 78.2 p.p.m. (δH 4.87 p.p.m.) were observed, respectively, whereas in the ^{13}C NMR spectrum of the new derivative **2**, the signal of C-33 was shifted to low field area and appeared at δC 207.70 p.p.m., and in ^1H spectrum the 33-CH signal disappeared. The multiplicity of the methyl signal 34-CH_3 in the ^1H NMR spectrum turned into the singlet δH 2.20 (δC 31.97 p.p.m.) and the signals of the methylene group 32-CH_2 were split into doublets of doublets δH 2.68 and 2.21 p.p.m. (δC 46.63 p.p.m.) with significantly increased shifts when compared with oligomycin A (**1**). The shifts of the 31-CH group (δH 4.21 p.p.m. and δC 68.10 p.p.m.) also increased according to the negative inductive effect of the 33-carbonyl group. Signals of the rest atoms in NMR spectra of **2** changed insignificantly, indicating that there were no other structural differences in molecule **2** in comparison with oligomycin A (**1**).

In addition, in our previous works,[11–13] signals of the atoms 7 and 11, 8 and 10 and 37 and 38 oligomycin A (**1**) were assigned ambiguously to an accuracy of reverse assignment. Now, on the basis of detailed analysis of ROESY (rotating-frame nuclear Overhauser effect correlation spectroscopy) and HMBC (heteronuclear multiple bond correlation) spectra, we can propose unambiguous assignment for oligomycin A (**1**) and their derivatives **2** and **3** (Supplementary Table S1 and Supplementary Figures S6–S11).

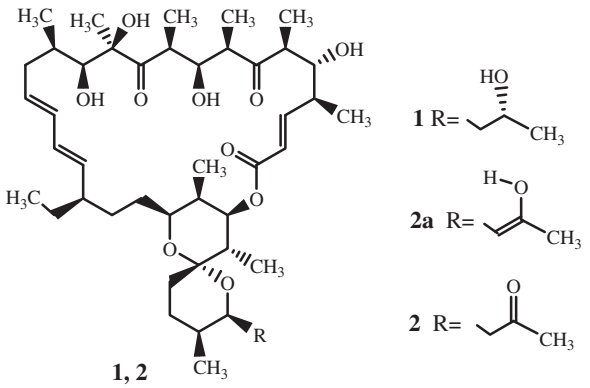

Figure 1 The described structures for the oligomycin A (**1**, **2a**, and **2**).

QCCs and docking studies

NMR data indicated that 33-dehydrooligomycin A (**2**) in solution has the side chain (R) that corresponded to a 2-propanone residue, whereas its enol form **2a** was not observed. To compare the relative stability of the 33C keto–enol tautomers of **2**, the theoretical quantum chemical calculations (QCCs) were used for the gas phase without modeling of solvation. QCCs were carried out using the software package Spartan-10 (https://www.wavefun.com/products/spartan.

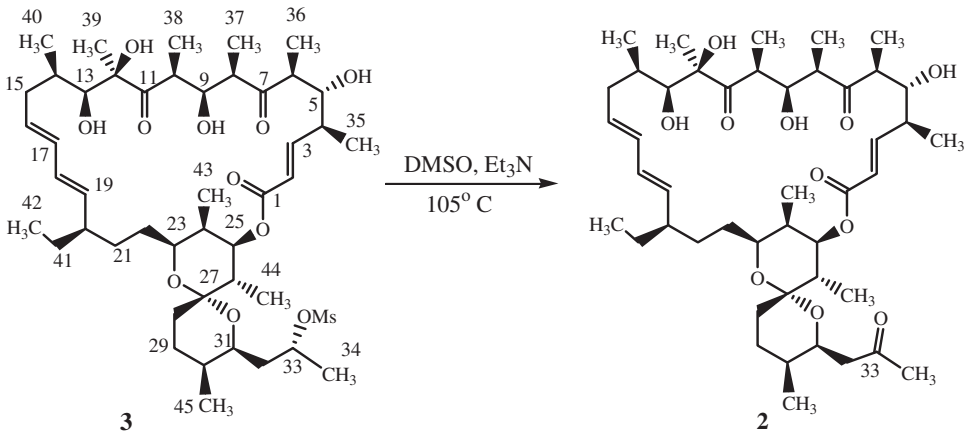

Scheme 1 Synthesis of 33-dehydrooligomycin A (**2**) from 33-*O*-mesyloligomycin A (**3**) by the Kornblum oxidation.

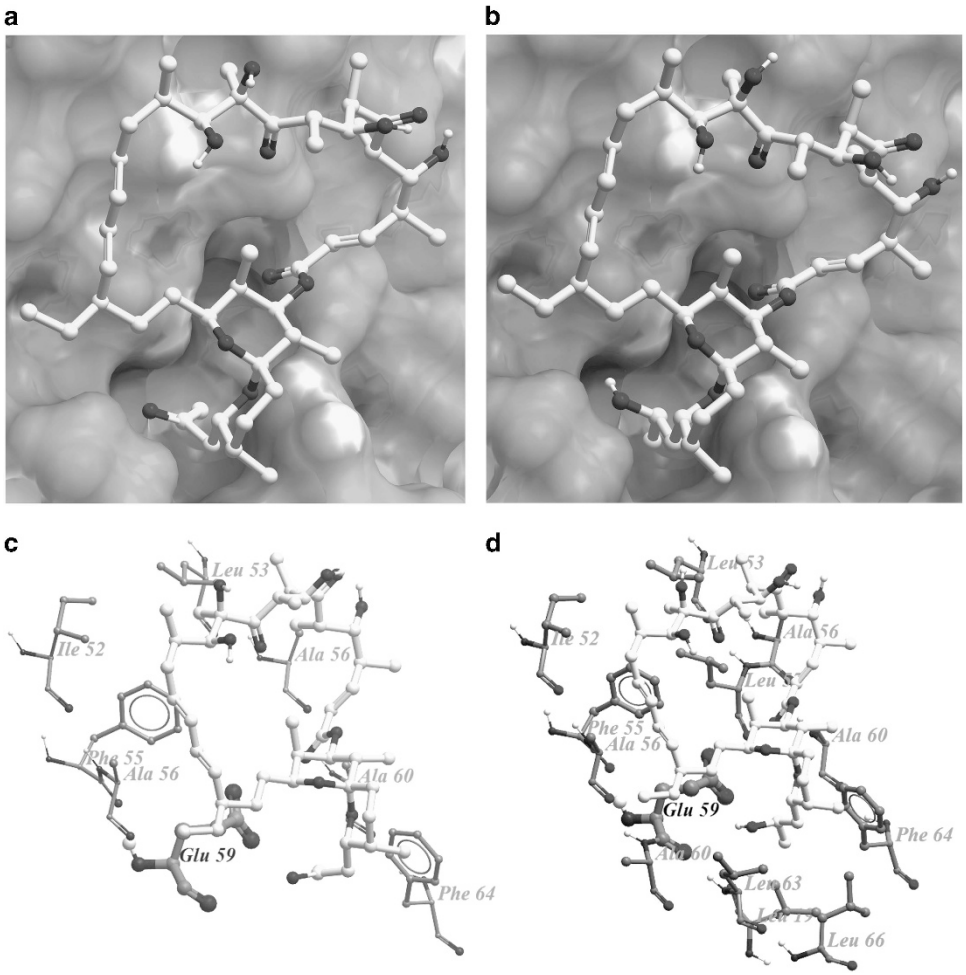

Figure 2 Structure of complexes 33-dehydrooligomycin A (**2**) and oligomycin A (**1**) with F_O subunit of ATP synthase, resulting docking using ICM-Pro. (**a**, **b**) Localization of the best binding energy conformations 33-dehydrooligomycin A and oligomycin A on the target surface. The hydrophobic regions on the surface of F_O subunit ATP synthase are painted in green, the donors of hydrogen bonds are in blue and acceptors in red. (**c**, **d**) The amino acid residues of F_O subunit of ATP synthase located in 3 Å radius vicinity of the best energy conformations of 33-dehydrooligomycin A (**2**) and oligomycin A (**1**). The 3D model atoms are painted in the following colors: carbon: yellow for the ligands and dark gray for the amino acids; oxygen atoms: red; nitrogen atoms: blue; and hydrogen atoms: white. For better clarity, it shows only the polar hydrogen atoms. A full color version of this figure is available at the *Journal of Antibiotics* journal online.

html) with full optimization of the geometric parameters of the structures by semiempirical PM6[19] and density functional B3LYP/6–31G**.[20] Calculation of normal vibration frequencies of the structures showed that they belong to the low potential energy surface.

Results of QCCs have shown that the keto form **2** is thermodynamically more stable for 7.5–8.2 kcal mol^{-1} (Supplementary Figure S12 and Supplementary Table S2), although the enolic form **2a** (Supplementary Figure S13) could be stabilized with an intramolecular hydrogen bond. The enolic form **2b** without an intramolecular hydrogen bond was less beneficial for 3.0–3.5 kcal mol^{-1} than **2a** (Supplementary Figure S14 and Supplementary Table S2). It should be noted that the predicted structure of enolic form **2a** was generally close to the structure issued for oligomycin A by Palmer *et al.*[8–10] based on their crystallographic data. The calculated length of hydrogen bond between enol hydroxyl and oxygen of the spiroketal moiety in **2a** reached 2.2 Å (PM6 method) or 1.9 Å (B3LYP/6–31G** method) and was slightly shorter than that determined from crystal data 2.4 Å.

Thus, results of QCC evaluation corresponded well with the NMR data for the resulting 33-dehydrooligomycin (**2**), both of which indicate that this derivative predominantly exists in the lower energy keto form **2** but not in the enol **2a** form, as observed by Palmer *et al.*[8–10]

Next, for prediction of biological potencies of novel 33-dehydrooligomycin A (**2**), comparative docking studies of **1** and **2** with F_O subunit of ATP synthase was performed by application of Molsoft ICM-Pro version 3.8-3 (Molsoft L.L.C., San Diego, CA, USA). Docking was carried out on the surface F_O subunit of the ATP synthase taken from PDB:4f4s. Comparing structures of the complexes of oligomycin A (**1**) from the PDB:4f4s and the best binding energy conformation obtained by ICM-Pro (Supplementary Figure S15) showed nearly identical localization of the antibiotic on a surface of the target. It indicates both ICM-Pro Software and the parameters were well suited for the simulation of the binding of oligomycin A (**1**) with the target, and were selected for the docking procedure that could be useful for its derivatives. Comparative analysis of the location geometry (Figure 2) and binding energy for 33-dehydrooligomycin A (**2**) (Table 1) and oligomycin A (**1**) led to several conclusions. The main contribution to the binding energy in the case of both molecules is from their hydrophobic components. It is caused by the fact (see Figure 2) that the area in which there is an interaction of the

ligands with the target, in the majority, consists of the acids having hydrophobic side groups in the structure. Modification of 33-hydroxyl group of **1** into the carbonyl of **2** appears to have led to change of a Coulomb contribution in binding energy. These significant changes could be explained in that an attraction between the 33-hydroxyl group of oligomycin A (**1**) and carboxyl of Glu59 resulted in the transformation into 33-keto group of **2** that was converted into the repulsion of the latter with the carboxy group of the target. Generally, although both antibiotics had shown similar binding with the target, results of the simulation predicted decreasing affinity of the F_O subunit of the ATP synthase to 33-dehydrooligomycin A (**2**) in a comparison with parental oligomycin A (**1**).

Biological activity of 33-dehydrooligomycin (2)

Finally, the antimicrobial properties and antiproliferative activities of 33-dehydrooligomycin A (**2**) in comparison with oligomycin A were evaluated. *In vitro* antifungal activity of 33-dehydrooligomycin A (**2**) was evaluated by broth microdilution-based assays[21,22] against yeasts strains *Candida* spp. (clinical isolates and reference strains) and filamentous fungus (*Aspergillus niger* 137a, *Trichophyton rubrum* 2002, *Microsporum canis* B-200). The reference strains of *Candida parapsilosis* ATCC 22019 and *Candida albicans* ATCC 24433 were obtained from the Collection of Pathogenic Microorganisms Tarasevich State Institute of Standardization and Control of Biomedical Preparations (Moscow, Russia).

The antifungal activities of 33-dehydrooligomycin A (**2**) in addition to the reference agents oligomycin A (**1**) and fluconazole against *Candida* spp. strains (both collection and clinical) are presented in the Table 3. It has been found that the fluconazole-resistant clinical isolates of *C. albicans* were also resistant to oligomycin A (**1**) and 33-dehydrooligomycin A (**2**). Against the *Candida krusei* strain, resistant to fluconazole, 33-dehydrooligomycin A (**2**) showed high activity closed to oligomycin A (**1**) (Table 2).

The *in vitro* antiactinobacterial activity was evaluated against *Streptomyces fradiae* ATCC 19609 strain that is supersensitive to oligomycin A (**1**). The MIC in liquid medium was not applicable for some actinobacteria including *Streptomyces*, as its culture forms pellets in liquid media, and hence the *in vitro* MICs of the 33-dehydroolygomycin A (**2**) and oligomycin A (**1**) against *S. fradiae* were determined by an agar dilution method. According to our data, **2** is approximately twice as weak than oligomycin A (**1**) against *S. fradiae* ATCC-19609 (Table 2). The strain *S. fradiae* ATCC 19609 is a convenient model for studying human F_1F_O ATP synthase because of the similarity of its subunit-c of the F_1F_O ATP synthase with subunit-c of the human F_1F_O ATP synthase.[23,24] As a result of this similarity, we can assume that the observed decreasing of activity of 33-dehydroolygomycin A (**2**) against *S. fradiae* may be related to the decreasing of affinity of the antibiotic to F_1F_O ATP synthase as shown by molecular modeling.

Finally, *in vitro* the cytotoxicity of 33-dehydrooligomycin A (**2**) was evaluated against human postnatal fibroblasts and cancer cell lines (Table 3) according to previously described methods.[25] We observed that 33-dehydrooligomycin A (**2**) was slightly more potent against the human leukemia cell line K-562 than oligomycin A (**1**). The proliferation of the cell line colon carcinoma cell line HCT116 was also inhibited by 33-dehydrooligomycin A (**2**) less potently. In the meantime the human postnatal fibroblasts were two times less sensitive to 33-dehydrooligomycin A (**2**) than to oligomycin A (**1**). Thus, the 33-dehydrooligomycin A (**2**) showed higher activity against leukemia cell cells when compared with oligomycin A (**1**), but was less cytotoxic for normal cells.

Table 1 Contributions (kcal mol^{-1}) of the best binding energy conformations (obtained with ICM-Pro3.8-3) into the energy of binding (Δ*Gbind*) 33-dehydrooligomycin A (2) and oligomycin A (1) with F_O subunit of ATP synthase

Ligand name	ΔG_{bind}	ΔG_{eq}	ΔG_{solv}	ΔG_{VdW}	$-\Delta TS$	ΔU
Oligomycin A (**1**)	−22.1	−1.5	2.0	−33.8	10.5	0.8
33-Dehydrooligomycin A (**2**)	−17.4	3.9	−0.1	−33.0	11.1	0.8

DISCUSSION

In this report, we have described for the first time the synthesis, physicochemical properties and biological evaluation of 33-dehydrooligomycin A (**2**). It is worth noting that the oxidation by the reporting scheme can be carried out probably for other antibiotics of the oligomycin–rutamycin group having similar 2-hydroxypropyl side chain. The antimicrobial properties against the new derivative **2** were similar or approximately twice as weak as the parent oligomycin A compound (**1**). It should be noted that this transformation of oligomycin A led to increased activity against the leukemia cell line K562 and decreased cytotoxicity against nonmalignant human fibroblasts. This indicated the expediency of in-depth evaluation of the spectrum of antiproliferative activity of 33-dehydrooligomycin A (**2**). In addition, the introduction of a reactive ketone group at position 33C of oligomycin A opened new opportunities for further synthetic and research studies.

Diminishing activity in several test cultures agreed well with results of molecular modeling of the interaction of **2** with the intracellular target, the c-subunit of the F_1F_O ATP synthase. Moreover, results of the docking studies by ICM-Pro Software shows that the predicted structures of the complex of oligomycin A (**1**) with the target were nearly identical to crystallography data. It indicated that ICM-Pro Software is a useful tool for the simulation of oligomycin binding with the target and for design of a new generation of semisynthetic oligomycin A derivatives.

Finally, NMR data for 33-dehydrooligomycin (**2**) in addition to results of QCCs have shown that this derivative preferentially exists in keto form **2** than in the enol tautomer **2a** that Palmer *et al.* previously proposed as a structure for oligomycin A. The question as to the existence of the enol for derivative **2** remains open for future studies, but it seems that Palmer's puzzle is a peculiarity of crystallographic analysis of this particular structure that could have arisen as a result of the mobility of the hydroxypropyl side chain of oligomycin A in crystals.

METHODS

General experiments

Oligomycin A (**1**) (purity 95%) was produced at Autonomous Non-Commercial Research Center of Biotechnology of Antibiotics BIOAN (Moscow, Russian Federation) using *S. avermitilis* NIC B62. Isolation and purification were performed by extraction with an acetone–hexane mixture, followed by crystallization. 33-*O*-Mesyl-oligomycin A (**3**) was prepared as described earlier.[12] All other reagents and solvents were purchased from Aldrich-Sigma (St Louis, MO, USA) and Merck (Darmstadt, Germany). The solutions were dried over sodium sulfate and evaporated under reduced pressure on a Buchi rotary evaporator at 40 °C. The progress reaction products, column eluates and all final samples were analyzed by TLC on Merck G60 F254-precoated plates. Reaction products were purified by column chromatography on Merck silica gel 60 (0.04–0.063 mm) cards.

Table 2 Antimicrobial activities (MIC μg ml^{-1}) of tested compounds

	MIC, μg ml^{-1}		
Microorganism	*Fluconazole*	*Oligomycin A (**1**)*	*33-Dehydrooligomycin A (**2**)*
C. parapsilosis ATCC 22019	4	2	4
C. albicans ATCC 24433	4	4	4
C. utilis 84	2	1	2
C. tropicalis 3019	2	1	2
C. glabrata 61 L	32	>32	>32
C. albicans 604 M (R)	>32	32	>32
C. albicans 80 (R)	>32	32	>32
C. krusei 432 M	>32	2	4
M. canis B-200	>32	2	2
T. rubrum 2002	>32	2	2
A. niger 137 a	32	0.5	2
S. fradiae ATCC19609	—	0.05	0.1

Table 3 Antiprolifertive activity (IC_{50}, μM) of oligomycin A (1) and 33-dehydrooligomycin A (2) against the human cancer cell lines and normal human fibroblasts

	IC_{50}, μM		
Compound	*K-562*	*HCT-116*	*HPF*
Oligomycin A (**1**)	0.21 ± 0.03	0.9 ± 0.2	3.8 ± 0.5
33-Dehydrooligomycin (**2**)	0.12 ± 0.01	3.4 ± 0.3	7.8 ± 0.2

HPLC analyses were performed on Shimadzu LC 20 AD instrument (Kyoto, Japan, Kromasil-100-5-mkm, C-18 column, 4.6 × 250 mm, MeCN–H_2O mixture). The percentage of MeCN had been increased from 70 to 95% within 10 min and then it had been kept 95% within 30 min at a flow rate of 1 ml min^{-1}.

HR-MS ESI spectra were recorded on a Bruker micrOTOF-Q II-MS instrument (Bruker Daltonics GmbH, Bremen, Germany). The samples were dissolved in methanol (0.10 mg ml^{-1}) and the solutions of the samples were injected directly into the ESI source by a syringe at a flow rate 3 μl min^{-1}. The mass spectrometer was operated under the following conditions: an endplate offset of −500 V, nebulizer pressure of 0.4 Bar, a drying gas flow rate of 4 l min^{-1} at 180 °C and a capillary voltage of −4.5 kV and 4 kV in the positive and negative ionization mode, respectively. The instrument was calibrated with a Fluka electrospray calibration solution (Sigma-Aldrich, Buchi, Switzerland) that was 100 times diluted with AcCN. The accuracy was better than 0.43 p.p.m. in a mass range between *m/z* 118.0862 and 2721.8948. All solvents used were purchased in best LC-MS qualities.

UV spectra were obtained on UV/VIS double beam spectrometer (UV-2804, UNICO, Dayton, NJ, USA).

IR spectra were recorded on Nicolet iS10 Fourier transform IR spectrometer (Nicolet iS10 FT-IR, Madison, WI, USA).

Optical rotations were measured on an Optical Activity AA-55 polarimeter (Optical Activity, Cambridgeshire, UK).

NMR spectra were recorded on a Bruker Avance 600 spectrometer with proton resonance frequency 600 MHz. For the substance, one-dimensional ^{1}H and ^{13}C NMR spectra were registered, as well as a series of two-dimensional spectra, namely ^{1}H–^{1}H scalar correlation COSY, ^{1}H–^{1}H space correlation ROESY and heteronuclear correlations ^{1}H–^{13}C HSQC (heteronuclear single quantum coherence) and ^{1}H–^{13}C HMBC. Approximately 10 mg of the substance was dissolved in 550 μl $CDCl_3$. The spectra were recorded at 298 K. Chemical shifts were measured in ^{1}H and ^{13}C spectra, relative to the signals of the solvent (deuterochloroform). Two-dimensional spectra were recorded on TXI (triple resonance inverse) probe with the pulsed field gradient. The COSY experiment was realized with double quantum filter. The gradient coherence selection with detection by the method of echo–antiecho was used for HSQC spectrum. A ROESY experiment was recorded with a mixing time of 300 ms.

Synthesis of the 33-dehydrooligomycin (2)

A stirring solution of 33-*O*-mesyl-oligomycin A (**3**;[12] 0.03 g, 0.034 mmol) and triethylamine (0.15 ml, 1.36 mmol) in dry DMSO (15 ml) was heated in argon atmosphere at 105 °C for 3 h. When the reaction was completed (TLC analyzed in hexane–acetone, 10:7), the resulting solution was cooled and quenched by adding 0.01 N HCl (10 ml). An aqueous solution was extracted with EtOAc (20 ml × 2). The combined organic layer was carefully washed with water (20 ml × 3) and brine (20 ml), dried with Na_2SO_4 and evaporated. The residue was purified by column chromatography on silica gel in hexane–acetone (10:7) and chloroform–methanol (10:0.5) to give 0.018 g (66.1%) of product **2** (86% purity) as a colorless amorphous powder. The crystallization from hexane–dichloromethane (10:1) gave 0.014 g (50%) of product **2** (96.1% purity).

Rf = 0.57 (hexane–acetone, 10:7); R_t = 16.59, 96.1% (Supplementary Figure S1); HRMS (ESI) $[M+Na]^+$ calculated for $C_{45}H_{72}NaO_{11}$: 811.4972, found: 811.4988. HRMS (ESI) $[M+K]^+$ calculated for $C_{45}H_{72}KO_{11}$: 827.4712, found: 827.4763 (Supplementary Figure S4); UV spectrum (MeOH) λ_{max} nm (log ε): 225 (4.05), 232 (4.02), 243 (3.85); IR $\nu_{max,}$ (film) cm^{-1} 3495, 2973, 2925, 2874, 1699, 1642, 1466, 1382, 1276, 1222, 1190, 1036, 1091, 1047, 984, 924, 879, 803, 686 (Supplementary Figure S3); $[a]_D^{20}$ −50° (c 0.2, MeOH); m. p. 119–120 ° C.

Molecular docking

The coordinates for the target 3D models were taken from PDB:4f4s. The 3D models of the ligands and the target were built using Molsoft IC-Pro version 3.8-3.[26] For creation of the target 3D model, the following procedures were performed: addition of the hydrogen atoms and missing heavy atoms in amino acids side groups; assignment of the atom types and the charges from force field ECEPP/3[27] for the targets and from Merck molecular force field[28] or the ligands; estimating charged states of all His, Asp, Glu, Arg, Lys and Cys in the proteins taking into account pH 7.0; imposition of internal coordinates tree on the original pdb coordinates; MM optimization by using conjugate gradient minimization was done to eliminate minor van der Waals clashes of the atoms. The procedure of flexible ligand docking was performed using above mentioned Molsoft ICM to define the most probable binding site of ligands on the target surface. Docking was carried out in two stages. Search for the most likely binding sites was carried out on the rigid targets in the first step. During the first procedure, only conformational, rotary and position mobility of the ligands were taken into account, and geometry of a target did not change. The target–ligand complexes obtained from the first rigid-body docking were further refined by optimizing of the conformation of amino acids side chains located in 4 Å radius vicinity of the ligand with application of the Biased Probability Monte Carlo (BPMC) procedure. Description of the binding energy scoring used in these stages and BPMC procedure is reported by and Totrov and Abagyan.[29] Finally, conformational stack obtained from refining docking procedure was sorted by energy, and 100 best conformations were taken to estimate the binding energy more precisely. The free energy of complex formation is calculated using the formula:

$$\Delta G_{\text{bind}} = \Delta G_{\text{eq}} + \Delta G_{\text{VdW}} + \Delta G_{\text{hbond}} + \Delta U - T\Delta S + \Delta G_{\text{solv}}$$

as the sum of the free energy of complexation in a vacuum and ΔG_{solv} the difference between the solvation energy of the complex and the sum of solvation energy of the unbound target and the ligand. Energy complex formation in vacuum was evaluated as the sum of change of electrostatic ΔG_{eq} and van der Waals ΔG_{VdW} components, energy of hydrogen bonds formation ΔG_{hbond}, strain energy of the bond, valence and dihedral angles ΔU and the change in entropy due to the loss of the conformational mobility of the

target and the ligand. Solvation energy was evaluated by the method of Wesson–Eisenberg.[30]

Antimicrobial assay

The *in vitro* antifungal activities against yeast and filamentous fungi were evaluated accordingly to the Reference Method for Broth Dilution Antifungal Susceptibility Testing of Yeasts [21] and Reference Method for Broth Dilution Antifungal Susceptibility Testing of Filamentous fungi.[22] All strains of clinical isolates used in this study were earlier obtained from the Collections of State Scientific Center of Antibiotics for antimicrobial activity. Strains of *Candida* spp. and spores of filamentous fungus were stored in medium supplemented with 10% (vol/vol) of glycerol at − 80 °C.

All strains were transferred onto the plates with Sabouraud Dextrose Agar (Oxoid, Basingstoke, UK) and cultured at 35 °C for 48 h for *Candida* spp., 3 days for *A. niger* and ~ 3 weeks for dermatophytes.

Suspensions of filamentous fungus spores and yeast cells were prepared to reach a concentration in the final inoculum equal to $0.5–2.5 \times 10^4$ spores per ml and 10^3 CFUs per ml, respectively. Stock solutions of each biologically active agent in medium (RPMI-1640) with glutamine, without bicarbonate and with the addition of glucose 2% w/v were used in serial twofold microdilutions. The individual samples were prepared in 100% DMSO (Merck, Darmstadt, Germany) at a starting concentration of 10 mg ml^{-1}. Finally, the sample stock solutions were then diluted in RPMI-1640 medium to obtain concentration of 64 μg ml^{-1} directly before using. Growth media consisting of oligomycin derivative (100 μl was added to each well) at concentrations ranging from 0.25 to 32 mg l^{-1} were then inoculated with 100 μl aliquots of the test microorganism (the final concentrations of DMSO in all samples were 0.32%). MIC was defined as the lowest concentration at which complete visible growth inhibition was detected after 24–48 h of incubation for *Candida* spp. and 48–72 h—for filamentous fungus. In addition, the fluconazole activity was also tested against *C. parapsilosis* ATCC 22019 strain as a quality control. Fluconazole MIC estimates were calculated as means and corresponded to the MIC ranges for reference *Candida* strain using CLSI macrodilution reference methods.

The *in vitro* antibacterial activities against *S. fradiae* ATCC 19609 were evaluated by an agar dilution method. The stock solutions of the test compounds were prepared in DMSO, and then the required concentrations ranging from 1 to 0.1 μg ml^{-1} were obtained by diluting the stock solution in cultural medium MG. Aliquots (1 ml) of cultural medium MG supplemented with 0.8% agar, *S. fradiae* spore suspensions (10^5 CFUs per ml) and the required concentration of the test compound were added on a Petri dish (5 ml) containing 4 ml of 2% agar medium MG with the same concentration of the test substance. Following incubation at 28 °C for 72 h, the MICs were determined as the lowest concentrations of antibiotic causing virtually complete inhibition of bacterial growth.

Cell culture and antiproliferative activity

The human colon carcinoma HCT-116 cell line (ATCC), the human myeloid leukemia K-562 cell line (ATCC) and the human postnatal skin fibroblast cell line were propagated in Dulbecco's modified Eagle's medium supplemented with 5% fetal calf serum, 2 mM L-glutamine, 100 units ml^{-1} penicillin and 100 μg ml^{-1} streptomycin at 37 °C, 5% CO_2 in a humidified atmosphere. Cells in logarithmic phase of growth were used in the experiments. Oligomycin A (**1**) and **2** were dissolved in DMSO as 10 mM stock solutions followed by serial dilutions in water immediately before experiments. The cytotoxicity was determined in a formazan conversion assay (3-(4,5-dimethylthiazol-2-yl)-2,5-diphenyltetrazolium bromide (MTT) test). Briefly, cells (5×10^3 in 190 μl of culture medium) were plated into a 96-well plate (Becton Dickinson, Franklin Lakes, NJ, USA) and treated with 0.1% DMSO (vehicle control) or with 10 μM of tested compounds **1** and **2** (0.10–50 μM; each concentration in duplicate) for 72 h. After completion of drug exposure, 50 μg of MTT was added into each well for an additional 2 h. Formazan was dissolved in DMSO, and the absorbance at 540 nm was measured. Cell viability at a given drug concentration (% MTT conversion) was calculated as the percentage of absorbance in wells with drug-treated cells to absorbance in wells with DMSO-treated cells (100%).

CONFLICT OF INTEREST

The authors declare no conflict of interest.

ACKNOWLEDGEMENTS

This study was supported by grants by the Russian Science Foundation (agreement no. 15-15-00141). We thank YN Luzikov for the help with NMR, NM Maliutina for HPLC and EN Bichkova (Gause Institute of New Antibiotics) for IR and UV analyses.

1 Smith, R. M., Peterson, W. H. & Mccoy, E. Oligomycin, a new antifungal antibiotic. *Antibiot. Chemother.* **4**, 962–970 (1954).
2 Symersky, J., Osowski, D., Walters, D. E. & Mueller, D. M. Oligomycin frames a common drug-binding site in the ATP synthase. *Proc. Natl Acad. Sci. USA* **109**, 13961–13965 (2012).
3 Carter, G. T. Structure determination of olygomycin A and C. *J. Org. Chem.* **51**, 4264–4271 (1986).
4 Morris, G. A. & Richards, M. S. Concerted use of two-dimensional NMR techniques in the *Ab initio* assignment of complex spectra: complete proton and carbon-13 assignment of oligomycin A. *Magn. Res. Chem.* **23**, 676–683 (1985).
5 Evans, D. A., Rieger, D. L., Jones, T. K. & Kaldor, S. W. Assignment of stereochemistry in the oligomycin, rutamycin, cytovaricin family antibiotics. Asymmetric synthesis of the rutamycin spiroketal synthon. *J. Org. Chem.* **55**, 6260–6268 (1990).
6 Panek, J. S. & Jain, N. F. Total synthesis of rutamycin B and oligomycin C. *J. Org. Chem.* **66**, 2747–2756 (2001).
7 Yang, P. W. *et al.* Oligomycin A and C, major secondary metabolites isolated from the newly isolated strain *Streptomyces diastaticus*. *Folia Microbiol.* **55**, 10–16 (2010).
8 Palmer, R. A. & Potter, B. S. X-ray Structures and absolute configurations of the antibiotics oligomycins A, B and C: inhibitors of ATP synthase. *J. Chem. Cryst.* **38**, 243–253 (2008).
9 Green, R. C. E. *et al.* A comparative study of the single crystal X-ray determination and molecular modelling of the binding of oligomycin to ATP synthase. *Comput. Biol. Chem.* **33**, 189–195 (2009).
10 Palmer, R. A., Ladd, M., Howlin, B. & Lisgarten, D. R. X-ray structures of two forms of the antibiotic oligomycin A: an inhibitor of ATP synthase. *Future Med. Chem.* **5**, 881–893 (2013).
11 Lysenkova, L. N. *et al.* Synthesis and anti-actinomycotic activity of thiocyanato derivative of oligomycin A modified in the side propanol residue. *Macroheterocycles* **8**, 424–428 (2015).
12 Lysenkova, L. N. *et al.* Synthesis and cytotoxicity of oligomycin A derivatives modified in the side chain. *Bioorg. Med. Chem.* **21**, 2918–2924 (2013).
13 Lysenkova, L. N. *et al.* Synthesis of 33-(*R,S*)-Bromo-33-deoxyoligomycin A. *Macroheterocycles* **9**, 307–313 (2016).
14 Omelchuk, O. A. *et al.* Synthesis and biological activity of 2,3,16,17,18, 19-hexahydrooligomycin A. *Macroheterocycles* **9**, 453–461 (2016).
15 Berdy, J., Aszalos, A., Bostian, M. & McNitt, K. *CRC Handbook of Antibiotic Compounds* **IV** (2) 319 (CRC Press, FL, USA, 1980).
16 Kornblum, N., Jones, W. J. & Anderson, G. J. A new selective method of oxidation. The conversion of alkyl halides and alkyl tosylates to aldehydes. *J. Am. Chem. Soc.* **81**, 1413–1414 (1959).
17 Krapcho, A. P. Dimethyl sulfoxide. *e-EROS Encyclopedia of Reagents for Organic Synthesis* doi:10.1002/047084289X.rd373.pub2 (2004).
18 Lysenkova, L. N. *et al.* Study on retroaldol degradation products of antibiotic oligomycin A. *J. Antibiot.* **67**, 153–158 (2014).
19 Stewart, J. J. P. Optimization of parameters for semiempirical methods V: modification of NDDO approximations and application to 70 elements. *J. Mol. Model.* **13**, 1173–1213 (2007).
20 Stephens, P. J., Devlin, F. J., Chabalowski, C. F. & Frisch, M. J. *Ab initio* calculation of vibrational absorption and circular dichroism spectra using density functional force fields. *J. Phys. Chem.* **98**, 11623–11627 (1994).
21 Clinical and Laboratory Standards Institute (CLSI). *Reference Method for Broth Dilution Antifungal Susceptibility Testing of Yeasts*third ednCLSI document M27-A3 (CLSI, Wayne, PA, USA, (2008).
22 Clinical and Laboratory Standards Institute (CLSI). *Reference Method for Broth Dilution Antifungal Susceptibility Testing of Filamentous fungi* 2nd ednCLSI document M38-A2 (CLSI, Wayne, PA, USA, 2008).
23 Alekseeva, M. G., Elizarov, S. M., Bekker, O. B., Lubimova, I. K. & Danilenko, V. N. F0 F1 ATP synthase of Streptomycetes: modulation of activity and oligomycin resistance by protein Ser/Thr kinases *Biochemistry* (Moscow). *Suppl. Series A Membrane Cell Biol.* **3**, 16–23 (2009).
24 Alekseeva, M. G. *et al.* FoF1-ATP synthase of *Streptomyces fradiae* ATCC 19609: structural, biochemical, and functional characterization. *Biochemistry (Mosc.)* **80**, 296–309 (2015).
25 Shchekotikhin, A. E. *et al.* The first series of 4,11-bis[(2-aminoethyl)amino]anthra[2,3-b]furan-5,10-diones: synthesis and anti-proliferative characteristics. *Eur. J. Med. Chem.* **46**, 423–428 (2011).

26 Abagyan, R., Totrov, M. & Kuznetsov, D. ICM, a new method for protein modeling and design: applications to docking and structure prediction from the distorted native conformation. *J. Comput. Chem.* **15**, 488–506 (1994).
27 Arnautova, Y. A., Jagielska, A. & Scheraga, H. A. A new force field (ECEPP-05) for peptides, proteins, and organic molecules. *J. Phys. Chem. B* **110**, 5025–5044 (2006).
28 Halgren, T. A. Merck molecular force field. I. Basis, form, scope, parameterization, and performance of MMFF94. *J. Comp. Chem* **17**, 490–519 (1996).
29 Totrov, M. & Abagyan, R. in *Drug-Receptor Thermodynamics: Introduction and Applications* (ed. R. B. Raffa) 603–624 (John Wiley & Sons, 2001).
30 Wesson, L. & Eisenberg, D. Atomic solvation parameters applied to molecular dynamics of proteins in solution. *Protein Sci.* **1**, 227–235 (Cambridge University Press, 1992).

Supplementary Information accompanies the paper on The Journal of Antibiotics website (http://www.nature.com/ja)